Characterizing Synchronized Lissajous Curves to Scrutinize Power Distribution Synchro-waveform Measurements

Milad Izadi, *Student Member, IEEE* and Hamed Mohsenian-Rad, *Fellow, IEEE*

Abstract—A new concept, called *synchronized Lissajous curve*, is proposed to study synchro-waveform measurements that are obtained from waveform measurement units (WMUs) in power distribution systems. Two types of synchronized Lissajous curves are discussed. The first one is created by plotting the *difference* of two synchronized voltage waveforms versus the *difference* of two synchronized current waveforms. The second one is created by plotting the difference of two synchronized voltage waveforms versus the difference of the *derivatives* of two synchronized current waveforms. These two curves carry valuable and *complementary* information about the state of the power system and the root cause of events and disturbances. We characterize the *area*, *rotational angle*, and *shape* of the introduced synchronized Lissajous curves to study events and disturbances in power distribution feeders.

Index Terms—Waveform measurement unit, WMU, synchronized Lissajous curves, substitution theorem, power distribution.

I. INTRODUCTION

WAVEFORM measurement units (WMUs) are new smart grid sensor technologies that provide time-synchronized voltage waveform and current waveform measurements [1], [2]. A typical WMU has a reporting rate of 256 to 512 samples per cycle; and a time accuracy of 1 μsec. Therefore, the waveform measurements from multiple WMUs are synchronized precisely; making them appropriate for the analysis of various disturbances in power distribution networks [3]. However, data availability in itself does not lead to enhanced grid intelligence. We need to translate the WMU data to insightful information.

In this paper, we address the above open problem by *characterizing* a new concept in power system monitoring; called *synchronized Lissajous curve*; which we first introduced in [4].

In general, a Lissajous curve is a graph that is constructed by plotting one waveform versus another waveform. Different types of Lissajous curves are traditionally used in signal and image processing; such as to analyze electrocardiogram and dielectric discharge [5]. Lissajous curves have occasional applications also in power engineering; such as to diagnose internal faults and winding deformations in power transformers [6]. Recently, we have extended the basic idea in the traditional Lissajous curves to introduce the novel concept of *synchronized* Lissajous curve in [4] to help us in studying the measurements from WMUs.

Our goal in this paper is to utilize the synchronized Lissajous curves to scrutinize events in power distribution systems.

The main contributions of this paper are as follows:

1) Two different types of Lissajous curves are introduced to facilitate the analysis of synchro-waveform measurements. The first one is obtained by plotting the *difference* of

The authors are with the Department of Electrical and Computer Engineering, University of California, Riverside, CA, USA; e-mails: {mizadi, hamed}@ece.ucr.edu. The corresponding author is H. Mohsenian-Rad.

two synchronized voltage waveforms versus the *difference* of two synchronized current waveforms. The second Lissajous curve is obtained by plotting the difference of two synchronized voltage waveforms versus the difference of the *derivatives* of two synchronized current waveforms.

2) It is shown that the two synchronized Lissajous curves carry valuable and complementary information about the waveforms that are captured by WMUs during events and disturbances; thus they can help us scrutinize the events.

3) The *characteristics* of the synchronized Lissajous curves during event conditions are investigated. Three key quantitative features are extracted, namely *area*, *rotational angle*, and *shape*. Through illustrative examples, the applications of each of these key features are investigated.

4) It is shown that the areas of the two synchronized Lissajous curves have physical meanings; as they resemble the weighted sum of active power and the weighted sum of reactive power, respectively. The areas can also be used to *detect* the event. The rotational angle of the synchronized Lissajous curves provide clear insight about the *location* of the event. The shape of the synchronize Lissajous curves help distinguish the *type* of the event or disturbance.

II. SYSTEM MODEL

Consider the power distribution feeder in Fig. 1(a). Suppose it is equipped with two WMUs, where WMU 1 is installed at the beginning of the feeder and WMU 2 is installed at the end of the feeder. Let $v_1(t)$ denote the voltage waveform and $i_1(t)$ denote the current waveform that are measured by WMU 1. Also, let $v_2(t)$ denote the voltage waveform and $i_2(t)$ denote the current waveform that are measured by WMU 2.

Together, WMU 1 and WMU 2 simultaneously monitor the feeder as a two-port network, as shown in Fig. 1(b). When an event or a disturbance occurs on the power distribution feeder, it may affect the voltage and current waveforms that are measured by WMU 1 as well as the voltage and current waveforms that are measured by WMU 2. The *relative* impact with respect to these two pairs of synchronized waveform measurements can reveal the characteristics of the event or disturbance. Therefore, next, we revise the two-port network model in Fig. 1(b) into a one-port network model in Fig. 1(c). Let us define:

$$v(t) = v_1(t) - v_2(t), \tag{1}$$

$$i(t) = i_1(t) - i_2(t), \tag{2}$$

as the *difference* between the synchronized voltage waveforms at WMU 1 and WMU 2, and the *difference* between the synchronized current waveforms at WMU 1 and WMU 2, respectively. By construction, $v(t)$ and $i(t)$ capture the *synchronized* nature
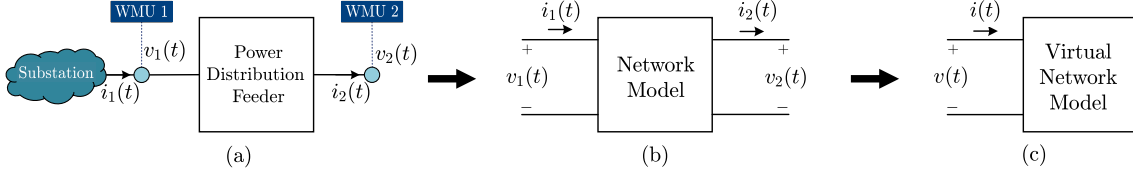
Fig. 1. System Model: (a) a distribution feeder that is equipped with two WMUs; (b) the equivalent two-port network; (c) the virtual one-port network.
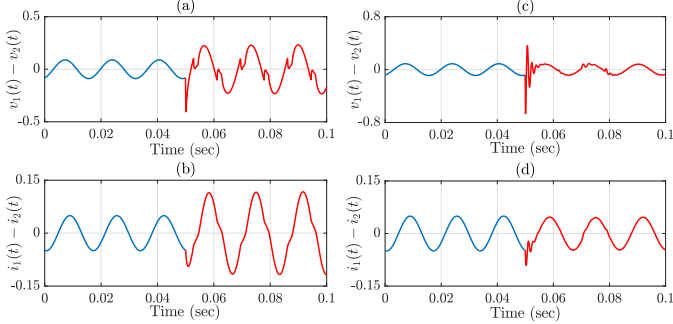

Fig. 2. Two examples of disturbances in power distribution that are represented by synchronized waveform measurements in (1) and (2): (a)-(b) high impedance fault; (c)-(d) capacitor bank switching. The normal conditions prior the disturbance are shown in blue; disturbance conditions are shown in red.

of the waveform measurements that are obtained by WMU 1 and WMU 2. The one-port network model is a *virtual* model. It can help us in discussing the concepts that we introduce in this paper. For example, consider the product $v(t)\, i(t)$. While this product may *not* be intuitive if it is defined based on the initial two-port physical network model in Fig. 1(b), it *is* intuitive when it is defined based on the one-port virtual network model in Fig. 1(c); because it simply denotes the instantaneous power that is injected into such *virtual* network model. Any other discussion involving the *difference* waveform measurements $v(t)$ and $i(t)$ can be similarly explained in the context of such virtual network model. The waveforms in (1) and (2) are in *per unit*; i.e., they are normalized to be comparable. Two examples for the captured waveforms are shown in Fig. 2.

Another waveform that we will use in this paper is created by taking the *derivative* of the current waveform in (2):

$$\frac{di(t)}{dt} = \frac{di_1(t)}{dt} - \frac{di_2(t)}{dt}. \tag{3}$$

We will use the above waveform in Section III-B.

III. Two Types of Synchronized Lissajous Curves

Consider the one-port virtual network model that we introduced in Section II. By construction, this network model requires access to *synchronized* waveform measurements. That is, in order to obtain $v(t)$ in (1), $i(t)$ in (2), and $di(t)/dt$ in (3), we need $v_1(t)$, $v_2(t)$, $i_1(t)$, and $i_2(t)$ to be time-synchronized; which is indeed the case when WMUs are being used.

We propose two types of *synchronized Lissajous curves* based on the waveforms in (1), (2), and (3). A Lissajous curve is obtained by plotting one waveform versus another waveform.

A. Lissajous Curve of $v(t)$ vs. $i(t)$

We can construct a synchronized Lissajous curve by plotting $v(t)$ versus $i(t)$. The synchronized Lissajous curves for the example waveforms in Fig. 2 are shown in Figs. 3(a) and (c).
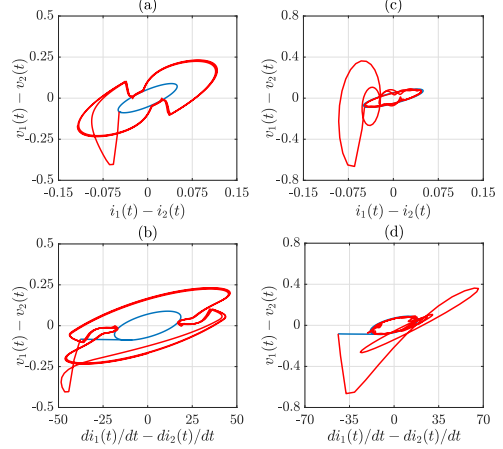

Fig. 3. The synchronized Lissajous curves of the waveforms in Fig. 2 under normal operating conditions (blue) and disturbance conditions (red): (a)-(b) high impedance fault; (c)-(d) capacitor bank switching.

B. Lissajous Curve of $v(t)$ vs. $di(t)/dt$

Another synchronized Lissajous curve can be constructed by plotting $v(t)$ versus $di(t)/dt$, where $di(t)/dt$ was defined as in (3). The synchronized Lissajous curves for the example waveforms in Fig. 2 are shown in Figs. 3(b) and (d).

IV. Analytical Characteristics

In this section, we investigate the fundamental characteristics of the two synchronized Lissajous curves that we introduced in Section III, and what they reveal about the events.

A. Area of the Synchronized Lissajous Curves

For the synchronized Lissajous curve that we introduced in Section III-A, we can define its area in each cycle T as follows:

$$Area_{v-i} = \left| \int_{i(t=0)}^{i(t=T)} v(t)\, di(t) \right|. \tag{4}$$

Similarly, for the synchronized Lissajous curve in Section III-B, we can define its area in each cycle T as follows:

$$Area_{v-di/dt} = \left| \int_{di(t=0)/dt}^{di(t=T)/dt} v(t)\, d\left(\frac{di(t)}{dt} \right) \right|. \tag{5}$$

The above areas can be obtained in *closed-form* during the *steady-state* conditions both before and after the event occurs. At steady-state conditions, we can express $v(t)$ and $i(t)$ as

$$v(t) = \sum_{h=1}^{H} V_h \cos(h\omega t + \theta_h), \tag{6}$$

$$i(t) = \sum_{h=1}^{H} I_h \cos(h\omega t + \gamma_h), \tag{7}$$

where ω is the fundamental rotational frequency; h is the harmonic order; V_h and θ_h are the magnitude and phase angle of the hth harmonic of the voltage waveform; I_h and γ_h are the

magnitude and phase angle of the hth harmonic of the current waveform; and H is the maximum number of harmonic orders.

From (4), (6), (7), we can obtain:

$$
\begin{aligned}
Area_{v-i} &= \left| \int_{t=0}^{T} \left(\sum_{h=1}^{H} V_h \cos(h\omega t + \theta_h) \right) \right. \\
&\qquad \left. \left(-\sum_{h=1}^{H} h\omega I_h \sin(h\omega t + \gamma_h) \right) dt \right| \\
&= \left| \sum_{h=1}^{H} (\pi h) \left(V_h I_h \sin(\theta_h - \gamma_h) \right) \right| = \sum_{h=1}^{H} \alpha_h |Q_h|,
\end{aligned}
$$
(8)

where for each $h = 1, \ldots, H$, $Q_h = V_h I_h \sin(\theta_h - \gamma_h)$ denotes reactive power and $\alpha_h = \pi h$ is a *unit-less* constant. From (8), the area of the synchronized Lissajous curve in Section III-A is the weighted summation of *reactive power Q_h* in all harmonic orders. Here, reactive power is defined based on $v(t)$ and $i(t)$, i.e., with respect to the *virtual* one-port network in Fig. 1(c).

From (5), (6), (7), we can similarly obtain:

$$
\begin{aligned}
Area_{v-di/dt} &= \frac{1}{T} \left| \sum_{h=1}^{H} (2\pi^2 h^2) \left(V_h I_h \cos(\theta_h - \gamma_h) \right) \right| \\
&= \frac{1}{T} \sum_{h=1}^{H} \beta_h |P_h|,
\end{aligned}
$$
(9)

where for each $h = 1, \ldots, H$, $P_h = V_h I_h \cos(\theta_h - \gamma_h)$ denotes active power and $\beta_h = 2\pi^2 h^2$ is a *unit-less* constant. From (9), the area of the synchronized Lissajous curve in Section III-B is the weighted summation of *active power P_h* in all harmonic orders. Here, active power is defined based on $v(t)$ and $i(t)$, i.e., with respect to the *virtual* one-port network in Fig. 1(c).

It is worth clarifying that the areas in (8) and (9) are *not* equal to reactive power and active power associated with $v(t)$ and $i(t)$. The expression in (8) is different from $Q = \sum_{h=1}^{H} Q_h$; and the expression in (9) is different from $P = \sum_{h=1}^{H} P_h$. In fact, here we have no reason to calculate P and Q; because they can be obtained directly from the raw waveform signals $v(t)$ and $i(t)$. Instead, the above analysis was meant to analytically answer the following question: *is there any physical meaning associated with the areas of the synchronized Lissajous curves?*

The area of the synchronized Lissajous curves can be used to distinguish normal conditions from event conditions. During normal operating conditions, the area of the curve remains more or less unchanged. However, once an event occurs, the area of the synchronized Lissajous curve may change drastically. For example, consider the synchronized Lissajous curve in Fig. 3(a). The profile of the area of this curve is shown in Fig. 4; before, during, and after an event. The area is calculated at each time instant t for the period of $t - T$ to t, i.e., during the previous cycle. We can see that the event has a clear signature in Fig. 4. The area fluctuates and rises increasingly from $t = 0.05$ sec to $t = 0.068$ sec, indicating that an event has occurred at time $t = 0.05$, which is indeed correct. A similar indicator can be defined also based on the profile of the area of the synchronized Lissajous curves in Fig. 3(b); i.e., based on the synchronized Lissajous curve that we defined in Section III-B.
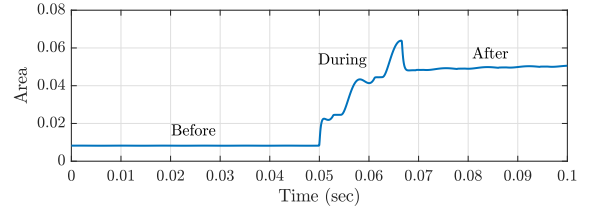

Fig. 4. An example for the area of the synchronized Lissajous curve (based on the definition in Section III-A), before, during, and after an event.

B. Rotational Angle of the Synchronized Lissajous Curves

Another important feature in the synchronized Lissajous curves is their *rotational angle*; which may indicate the location of the event. For example, consider the synchronized Lissajous curves in Fig. 5. They all represent *the exact same event*, i.e., a high impedance fault. However, the location of the fault is different in these three cases. While the shapes of the curves are similar, there are *rotational differences* among these figures; which are caused due to the different locations of the fault. When the fault occurs near the feeder hear, i.e., near WMU 1, the voltage drop between the two WMUs is smaller. This results in a smaller rotational angle, see Fig. 5(a). However, when the fault occurs near the end of the feeder, i.e., near WMU 2, the voltage drop between the two WMUs is larger. This results in a larger angle between voltage and current in the synchronized Lissajous curve, see Fig. 5(c). Note that, the fault current is almost the same in all the three fault cases in this example.

C. Shape of the Synchronized Lissajous Curves

In addition to the area and angle, the actual shape of each synchronized Lissajous curve can too draw a picture about the state of the power system and the root cause of the disturbance. During a *normal* operating condition, the synchronized waveforms in (1), (2), and (3) are all purely sinusoidal. Thus, (6) and (7) include only the *fundamental* components and we have:

$$
v(t) = V_1 \cos(\omega t + \theta_1), \tag{10}
$$

$$
i(t) = I_1 \cos(\omega t + \gamma_1). \tag{11}
$$

In that case, we can model the synchronized Lissajous curve in Section III-A as an *ellipse*, as follows [4]:

$$
Av(t)^2 + Bv(t)i(t) + Ci(t)^2 + D = 0, \tag{12}
$$

where $A = 1/V_1^2$, $B = -2\cos(\theta_1 - \gamma_1)/V_1 I_1$, $C = 1/I_1^2$, $D = -\sin^2(\theta_1 - \gamma_1)$. We always have: $B^2 - 4AC < 0$.

We can similarly model the synchronized Lissajous curve in Section III-B as an ellipse. The equations are omitted here.

Synchronized Lissajous curves always start from an ellipse during normal conditions; and deviate to other shapes depending on the type of the event. For example, for the case of the high impedance fault in Figs. 3(a) and (b), the shape of the synchronized Lissajous curves is affected by the presence of harmonics of odd orders in the fault current. As another example, for the case of the capacitor switching in Figs. 3(c) and (d), the synchronized Lissajous curves oscillate and then reach new steady state conditions in the shape of a new ellipse.

Therefore, the shape of the synchronized Lissajous curves can be used to distinguish the *type* of an event. This can be done
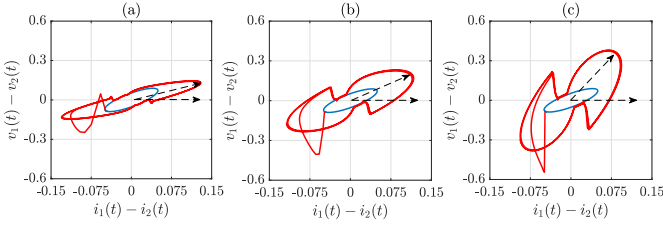
Fig. 5. The angle (marked with dashed arrows) in the synchronized Lissajous curves during the same event that occurs at three different buses: (a) near WMU 1; (b) in the middle of WMU 1 and WMU 2; (c) near WMU 2.
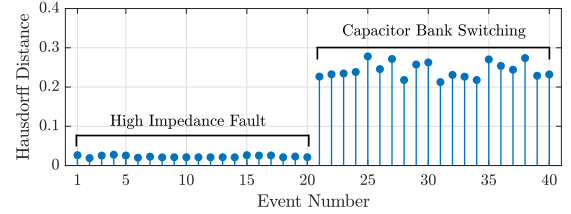

Fig. 6. The Hausdorff distance between the synchronized Lissajous curve of an *unknown* event with the synchronized Lissajous curves of 40 different *known* events, i.e., 20 high impedance faults and 20 capacitor bank switching events.

by examining the similarity/dissimilarity of the synchronised Lissajous curves among various events. This can be done, for example, by using the Hausdorff distance [7]. Consider two synchronized Lissajous curves that are obtained during two events. Γ denote the set of all the points on the Lissajous curve of the first event. Also let Λ denote the set of all the points on the Lissajous curve of the second event. The Hausdorff distance between the two Lissajous curves is defined as:

$$F(\Gamma, \Lambda) = \max\left\{f(\Gamma, \Lambda), f(\Gamma, \Lambda)\right\}, \quad (13)$$

where

$$f(\Gamma, \Lambda) = \max_{a \in \Gamma} \min_{b \in \Lambda} ||a - b||, \quad (14)$$

$$f(\Gamma, \Lambda) = \max_{b \in \Lambda} \min_{a \in \Gamma} ||b - a||, \quad (15)$$

where a and b are the points in set Γ and set Λ, respectively. If the shape of two synchronized Lissajous curves are *similar*, then their Hausdorff distance is close to zero, indicating that the two events are of the same type. Conversely, if the shape of two synchronized Lissajous curves are considerably *different*, then their Hausdorff distance is considerably greater than zero, indicating that the two events are of different types.

To asses the performance of the proposed index; suppose we have an event whose type is *not* known to us. Suppose we generate a total of 40 events; which include 20 events that are all high impedance faults; and another 20 events that are all capacitor bank switching events. Without loss of generality, we use the synchronized Lissajous curve that we introduced in Section III-A. Fig. 6 shows the Hausdorff distance between the unknown event and each of the 40 known events. The Hausdorff index is very small between the unknown event and events 1 to 20. However, the Hausdorff index is very large between the unknown event and events 21 to 40. Therefore, we can conclude that the unknown event is indeed a high impedance fault.

D. Applications of the Identified Characteristics

Based on the analysis in Sections IV-A to IV-C, each of the three key characteristics of the synchronized Lissajous curves can be used for various power system monitoring applications:

- The *area* of the synchronized Lissajous curve can be used for *event detection*. Once an event occurs, the area of the synchronized Lissajous curve changes sharply, as we saw in Section IV-A. Therefore, the *changes* in the area of the synchronized Lissajous curve can serve as an index to distinguish normal conditions from event conditions.

- The *rotational angle* of the synchronized Lissajous curve can be used for *event location identification*. As we saw in Section IV-B, if the event occurs near the feeder head, then the rotational angle of the synchronized Lissajous curve is

smaller. If the event occurs near the end of the feeder, then the angle of the synchronized Lissajous curve is *larger*.

- The *shape* of the synchronized Lissajous curve can be used for *event type identification*. During normal conditions, the shape of the synchronized Lissajous curve is an ellipse. Once an event occurs, the shape of the curve changes based on the *type* of the event. As we saw in Section IV-C, we can use the Hausdorff distance, or other methods in image processing, to distinguish different types of events.

V. CONCLUSIONS

A new graphical method, based on the concept of synchronized Lissajous curves, is proposed to scrutinize power distribution synchro-waveform measurements. The characteristics of the synchronized Lissajous curves, namely *area*, *rotational angle*, and *shape*, are studied both analytically and through examples. It is shown that, the *areas* of the two synchronized Lissajous curves resemble a notion of reactive power and a notion of active power, respectively. Therefore, the two synchronized Lissajous curves provide *complementary* insight about the WMU measurements. The *rotational angle* of the synchronized Lissajous curves further provides information about the location of the event. Finally, the *shape* of the synchronized Lissajous curves indicate the type of the event. The analysis in this paper can shed light on a new class of data-driven techniques that work based on the synchronized Lissajous curves and their characteristics for the use in various emerging applications, such as event detection, event localization, and event classification.

REFERENCES

[1] A. F. Bastos, S. Santoso, W. Freitas, and W. Xu, "Synchrowaveform measurement units and applications," in *Proc. IEEE PES General Meeting*, Atlanta, GA, USA, 2019, pp. 1–6.

[2] M. Izadi and H. Mohsenian-Rad, "Event location identification in distribution networks using waveform measurement units," in *Proc. IEEE PES ISGT Europe*, the Hague, Netherlands, 2020, pp. 924–928.

[3] M. Izadi and H. Mohsenian-Rad, "Synchronous waveform measurements to locate transient events and incipient faults in power distribution networks," *IEEE Trans. Smart Grid*, pp. 1–12, *Accepted for Publication*, May 2021.

[4] M. Izadi and H. Mohsenian-Rad, "A synchronized Lissajous-based approach to achieve situational awareness using synchronized waveform measurements," in *Proc. IEEE PES General Meeting*, Washington, DC, USA, 2021, pp. 1–5.

[5] D. Karacor, S. Nazlibilek, M. H. Sazli, and E. S. Akarsu, "Discrete Lissajous figures and applications," *IEEE Trans. Instrum. Meas.*, vol. 63, no. 12, pp. 2963–2972, Dec. 2014.

[6] A. Abu-Siada and S. Islam, "A novel online technique to detect power transformer winding faults," *IEEE Trans. Power Deli.*, vol. 27, no. 2, pp. 849–857, Apr. 2012.

[7] D. P. Huttenlocher, G. A. Klanderman, and W. J. Rucklidge, "Comparing images using the hausdorff distance," *IEEE Trans. Pattern Anal. Mach. Intell.*, vol. 15, no. 9, pp. 850–863, Sep. 1993.